Proceedings of The 2020 IEEE International
Conference on Real-time Computing and Robotics
September 28-29, 2020

A Sample-Based Color Correction Method for Laparoscopic Images

Longfei Wang, Qi Li, Haozhe Yang, Jia Huang, and Kai Xu*, *Member, IEEE*

***Abstract*— Color accuracy of endoscopic and laparoscopic images is of paramount importance for diagnosis and therapy during vision-guided minimally invasive surgery (MIS). However, unsatisfactory lighting conditions would increase the color difference of endoscopic and laparoscopic images. Aiming at improving the color accuracy of the images, a color correction matrix (CCM) can be utilized to transform the tristimulus values of the images to the new ones that are closer to the RGB values of standard color charts. But, a CCM is often related to a fixed illuminance, since the imaged tristimulus values of the same object vary under different illumination. Therefore, to improve the applicability of the CCM method under different illuminance conditions, a dynamic CCM method depending on the image luminance is needed. This paper hence presents a sample-based method that adjusts the CCM's implementation and extends its application for diverse illuminance, particularly in the low-illuminance scenario. The principal idea of the presented method is to correct an image's color under its average relative luminance using an interpolated CCM. The interpolated CCM is calculated from dozens of sample images of a color chart under different illuminance with respect to the images' average relative luminance. And the legitimacy of the interpolated CCM is based on an investigation of the correlation between the obtained CCMs. The experiments were performed on a laparoscope with two high-definition (HD) cameras, and the validations of color correction were conducted on the laparoscopic images captured for both standard color charts and abdominal models, demonstrating the effectiveness of the proposed approach.**

I. Introduction

Vision guidance plays an important role in robotic Minimally Invasive Surgery (MIS) [1]. Surgeons perform diagnosis and treatment relying on the visual feedback from the endoscopic and laparoscopic cameras during operations. In this case, clear images with accurate colors are essential for the information perception, such as organ distinction, blood vessels identification, and lesion recognition [2]. In reality, there would be undesired color differences between those in vivo and the images captured from an endoscope or a laparoscope. An important reason for the color discrepancy is unsatisfactory illumination [3].

This work was supported in part by the National Key R&D Program of China (Grant No. 2017YFC0110800), and in part by the National Natural Science Foundation of China (Grant No. 51722507).

Longfei Wang, Qi Li, Haozhe Yang are with the State Key Laboratory of Mechanical System and Vibration, School of Mechanical Engineering, Shanghai Jiao Tong University, Shanghai, China (e-mails: longfei.wang@sjtu.edu.cn, liqi362202@sjtu.edu.cn and silence1004@sjtu.edu. cn).

Jiang Huang is with Shanghai Lung Cancer Center, Shanghai Chest Hospital, Shanghai Jiao Tong University, Shanghai, China (e-mail: huangjiadragon@126.com).

Kai Xu is with the State Key Laboratory of Mechanical System and Vibration, School of Mechanical Engineering, Shanghai Jiao Tong University, Shanghai, China (corresponding author, phone: 86-21-34206547; e-mail: k.xu@sjtu.edu.cn).

Generally, there are two ways of illumination for an endoscope or laparoscope. One approach is to integrate a light source (e.g., light-emitting diode) to the tip of the endoscope. This approach suffers from the concentrated heating problem at the endoscope tip, due to the low photoelectric conversion efficiency. Another approach, which is more widely adopted, is to use an external light source and transmit the light to the endoscope tip via optical fiber. However, the transmission distance via optical fiber will decrease the illumination intensity and lead to spectral shift [4], increasing the color discrepancy of the captured images.

To ensure a satisfactory lighting condition for the endoscope, Sousa *et al* [5] proposed a dynamic illumination control scheme. But the proposed closed-loop control for image lighting adjustment took about 1 s and may be considered slow for real-time adjustment. Hence, dynamic adjusting the illumination for an endoscope to reduce the difference between the imaged color and the actual color of the captured object may be difficult due to unavailable hardware support.

A more widely-adopted approach for improving the color accuracy of the images is to regulate the images' tristimulus values to the ones that better present the actual colors. Khan *et al* [6] proposed a look-up table (LUT) method to better present the colors of the endoscopic images. However, this approach requires a pre-collected image database of different themes taken from different anatomical locations. It is more suitable for endoscopic images that do not change drastically from esophagus to intestines. In the intended laparoscopic applications, the images change more drastically. The color correction method in [7] used a neural network that is trained by the collected images of known standard color charts (the Munsell grey chips). However, the images used in the training set were captured under fixed camera positions and lighting conditions. If the lighting condition varies, the method will not be directly applicable. Another adopted method is the polynomial color correction (PCC) [8]. The PCC method calculates the target tristimulus values using a non-linear transformation on a constructed vector, where the number of elements in the vector depends on the degree of the polynomial (e.g. a 2-degree polynomial can be represented by $[R\ G\ B\ R^2\ B^2\ G^2\ RG\ RB\ GB]$). However, while the RGB is scaled by the surface radiance k, this method's effectiveness will be decreased, since the components of the 2-degree polynomial will be scaled by k or k^2. To solve that problem, a root-PCC (RPCC) was proposed in [9]. The RPCC method takes the n^{th} root of n-degree polynomial terms. The influence of the surface radiance is hence removed and the number of the terms in polynomial is changed (e.g. a 2-degree RPCC polynomial is given by $[R\ G\ B\ \sqrt{RG}\ \ \sqrt{RB}\ \ \sqrt{BG}\ ]$). However, as a nonlinear method, the computational demand for the RPCC method is relatively high.

978-1-7281-7293-4/20/$31.00 © 2020 IEEE

In comparison with the PCC and the RPCC methods, the least-square color correction matrix (CCM) method [10] is simpler, fast and can correctly map the imaged tristimulus values to the target values when the scene radiance or exposures changed. To improve the performance of CCM method, Finlayson *et al* [11] consider the shading profile into the CCM calculation, which also shows effectiveness in reducing the image color discrepancy.

However, illuminance variation still influences the effectiveness of the CCM method. Moreover, even when a fixed illumination is applied, the luminance on the captured images is also affected by the distance from the light source to the object surface. Therefore, in order to adapt the CCM method to a wide range of illuminance, a dynamic CCM method based on the image luminance is needed.

Hence, this paper presents a sample-based method that modifies the CCM's implementation and extends its application to situations with diverse illuminance. First, the sample images of a transmissive color target chart were captured from the laparoscopic with two HD cameras (as shown in Fig.1). Then, the CCMs for the sample images are calculated. Subsequently, the relationship between the average relative luminance of the images and the CCMs is established. With the sample CCMs and the relationship, the CCM for an image caught at any illuminance could be obtained by interpolating the sampled CCMs. Finally, the color of the image is corrected via the interpolated CCM. To validate the effectiveness, the CIE LAB color difference ΔE^*_{ab} [12] was evaluated to verify the proposed color correction approach.

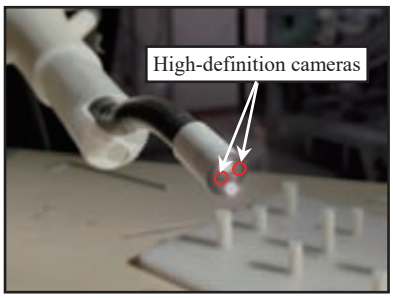

Figure 1. The laparoscope with two high-definition (HD) cameras.

This paper is organized as follows. Section II describes the calculation of the CCMs and establishes the relation between the CCMs and the image's average relative luminance. The experiments are reported in Section III, while the conclusions and future works are summarized in Section IV.

II. Principles And Analysis

The relationship between the CCMs and the images' average relative luminance shall be established. Firstly, the calculation of the CCM for a sample image is presented in Section II.A. Secondly, the relationship between the sample CCMs and the illuminance under which the sample images were captured is elaborated in Section II.B. Then, to correlate the average relative luminance of an image to a suitable CCM, the average relative luminance of the captured sample images was fitted with respect to the used illuminance, as reported in Section II.C. The evaluation of the color difference is briefly introduced in Section II.D.

A. CCM Calculation

The CCM method for image color correction referring to [10] uses the reference colors and correspondingly detected colors of a transmissive color target chart. The reference colors are designated as $\mathbf{C}_r \in \Re^{24\times3}$, while the detected colors are designated as $\mathbf{C}_d \in \Re^{24\times3}$, respectively, since there are 24 color blocks on the color target chart, referring to Fig. 2(c). The linear transformation matrix $\mathbf{M} \in \Re^{3\times3}$, which is the CCM matrix that maps $\mathbf{C}_d$ to $\mathbf{C}_r$, is defined as follows.

$$\mathbf{C}_r = \mathbf{C}_d \cdot \mathbf{M} \tag{1}$$

Then, $\mathbf{M}$ is given by Eq. (2).

$$\mathbf{M} = \left[\mathbf{C}_d{}^{\mathrm{T}}\mathbf{C}_d\right]^{-1}\mathbf{C}_d{}^{\mathrm{T}}\mathbf{C}_r \tag{2}$$

In order to reduce the influence from the possible outliers among the detected colors, a cost function $f(\mathbf{e})$ that is inversely proportional to the Euclidean distance $\mathbf{e} = \mathbf{C}_r - \mathbf{C}_d\mathbf{M}$, is used in Eq. (4).

$$f(\mathbf{e}) = diag\left(\left(\frac{|\mathbf{e}+\varepsilon|}{\mathbf{e}+\varepsilon}\right)^2\right) \tag{3}$$

Where $diag(1/\mathbf{x})$ means a diagonal matrix formed for a vector $\mathbf{x}$ whose diagonal element is the inverse of the $\mathbf{x}$'s corresponding element; ε is a small positive number avoiding division by zero.

Then, a better estimation of $\mathbf{M}$ can be written as in Eq. (4).

$$\mathbf{M} = \left[\mathbf{C}_d{}^{\mathrm{T}} \cdot f(\mathbf{e}) \cdot \mathbf{C}_d\right]^{-1}\mathbf{C}_d{}^{\mathrm{T}} \cdot f(\mathbf{e}) \cdot \mathbf{C}_r \tag{4}$$

Repeating Eq. (3) to Eq. (4), the optimized $\mathbf{M}$ will be obtained when the color error $\mathbf{e}$ is below a threshold. In this paper, the threshold is set at 1×10^{-4}.

B. Relationship between CCMs and Illuminance

The illuminance can have a severe impact on the detected color of the image and consequently affects the CCM. Hence, the CCM is only valid under a fixed illuminance. However, the illumination condition for a laparoscopic procedure is usually not constant. In order to establish a dynamic relation between the CCM and the illuminance L, a sample-based method was proposed to correlate the CCM and illuminance.

The calculated CCM of a sample image captured at illuminance L is denoted by $\mathbf{M}(L)$. The images of the transmissive color target chart that is shown in Fig.2(c) were captured by the laparoscopic cameras under different and uniform illumination generated by the adjustable lightbox that is shown in Fig.2(a) in a dark room. The test scenario is shown in Fig.2(b).

The CCM matrix $\mathbf{M}(L_j)$ is obtained under the j-th level of illuminance, ranging from 200 lx to 16000 lx, using the derivations detailed in Section II.A.

The correlation between the CCMs under the discretely changed illuminance L_j was examined using the Pearson correlation coefficients [13] as follows.

$$coef(\mathbf{v}_1, \mathbf{v}_2) = \mathrm{cov}(\mathbf{v}_1, \mathbf{v}_2) / \sqrt{\mathrm{var}(\mathbf{v}_1) \cdot \mathrm{var}(\mathbf{v}_2)} \tag{5}$$

Where $\mathrm{var}(\mathbf{v}) = \frac{1}{m}\sum_{k=1}^{m}(v_k - \tilde{v})^2$ with $\tilde{v} = \frac{1}{m}\sum_{k=1}^{m} v_k$ and $\mathrm{cov}(\mathbf{v}_1, \mathbf{v}_2) = \frac{1}{m}\sum_{k=1}^{m}(v_{1k} - \tilde{v}_1)(v_{2k} - \tilde{v}_2)$.

Since the CCM Matrix **M** comprises the tristimulus color correction vectors, the correlation among $\mathbf{M}(L_j)$ can be evaluated by the aforementioned correlation between the color correction vectors. Figure 3 shows the correlation coefficients between the correction vectors (the r/g/b vectors) of $\mathbf{M}(L_{j-1})$ and those of $\mathbf{M}(L_j)$. L_{j-1} and L_j can vary between 200 lx and 16000 lx.

From Fig.3(a), it can be found that the correlation coefficients between the r/g/b correction vectors of $\mathbf{M}(L_{j-1})$ and those of $\mathbf{M}(L_j)$ is close to 1, when $L_j \geqslant$ 4000 lx. $\mathbf{M}(L_{j-1})$ and $\mathbf{M}(L_j)$ are the adjacent CCMs and L_j is always one level higher in terms of illuminance (brighter) in this paper. Furthermore, the correlation coefficients between the r/g/b correction vectors of each $\mathbf{M}(L)$ and those of $\mathbf{M}_A$ are also plotted in Fig. 3(a), when $L \geqslant$ 4000 lx. $\mathbf{M}_A$ is the average of the CCMs with the lightbox illuminance more than 4000 lx. According to Fig. 3(a), $\mathbf{M}_A$ is chosen to represent the CCM when $L \geqslant$ 4000 lx.

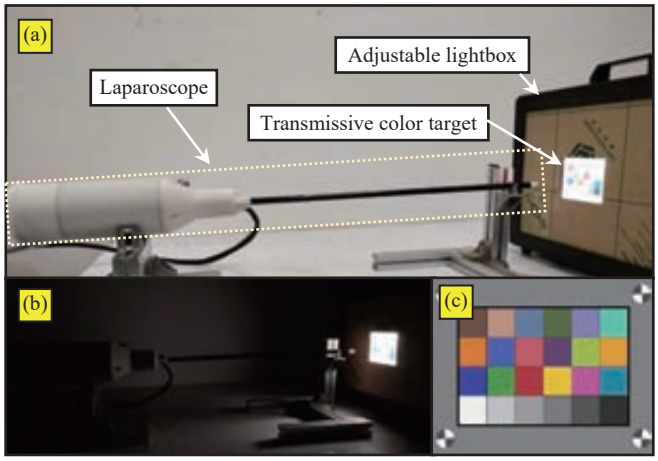

Figure 2. Laparoscopic sample images capturing: (a) the hardware used to capture sample images, (b) the practically dark scene for catching sample images, (c) transmissice color target

When L < 4000 lx, the correlation between the r/g/b correction vectors of $\mathbf{M}(L)$ and $\mathbf{M}(4000lx)$ varies as shown in Fig.3(b). But the correlation close to 1 between the r/g/b correction vectors of the CCMs with adjacent level of illuminance was noticed, when the illuminance increment is reduced to 200 lx. A linear interpolation for the CCM was hence adopted for L < 4000 lx.

Finally, the CCM is represented as follows, with respect to the level of illuminance.

$$\mathbf{M}(L_x) = \begin{cases} \mathbf{M}(L_j) - \dfrac{L_j - L_x}{L_j - L_{j-1}}\left(\mathbf{M}(L_j) - \mathbf{M}(L_{j-1})\right), & L_x < 4000lx \\ \mathbf{M}_A, & L_x \geq 4000lx \end{cases} \quad (6)$$

Where L_{j-1} and L_j are the two illuminance levels adjacent to L.

C. Relating the Average Relative Luminance and the CCMs

An image's luminance level can still vary even under the same illuminance due to many factors, such as scene distances. The average relative luminance of an image is designated as Y_A, which indicates the average pixel luminance in an image. The relation between Y_A and the CCMs can be established based on the relation between the lightbox illuminance L and the image luminance Y_A.

In order to obtain the Y_A, the color information of the image should be converted from RGB to another color space which contains the luminance dimension, such as CIE LAB, CIE LUV [12], YUV, YCrCb, et al. Selection of the color space does not affect the result, since our purpose is to find a relationship that can be used to determine the Y_A according to the lightbox illuminance L. The Y_A can then be directly obtained via the luminance dimension. In this paper, the RGB values of the laparoscopic images are converted into the YUV color space. The equation for calculating the luminance dimension Y of a pixel is as follows, referring to [14].

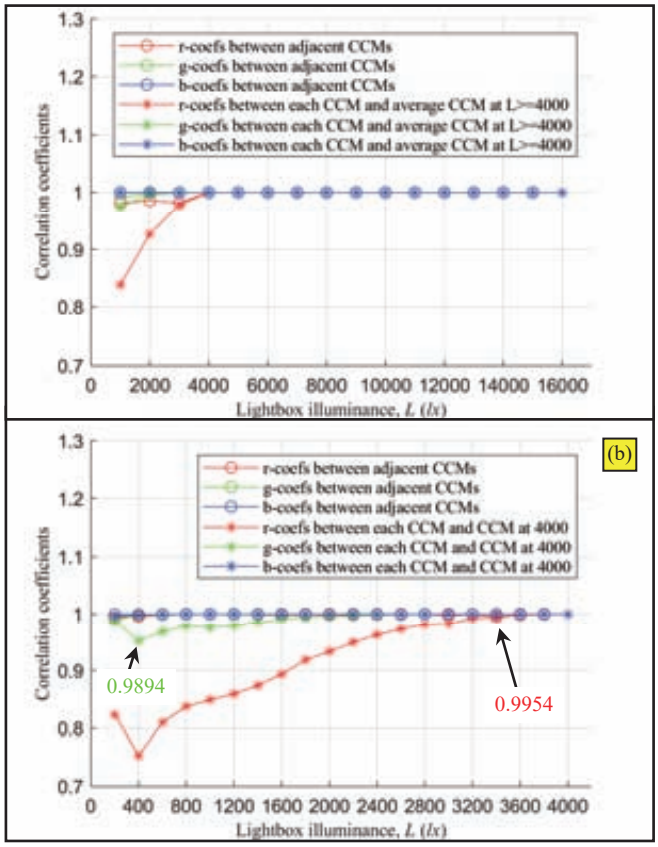

Figure 3. Correlation coefficients between the CCMs calculated from the captured images under different illuminance: (a) the illuminance ranging from 1000 lx to16000 lx, (b) the illuminance ranging from 200 lx to 4000 lx

$$Y = 0.299R + 0.587G + 0.114B \quad (7)$$

Where the RGB ranges are normalized to [0,1].

For an image of m-by-n, the calculation of Y_A is given by Eq. (8).

$$Y_A = \frac{1}{m \cdot n} \sum_{r=1}^{m} \sum_{c=1}^{n} Y_{r,c} \tag{8}$$

Where $Y_{r,c}$ is defined as the luminance Y value of a pixel in the YUV color space at the (r,c) point in the image coordinate.

To obtain the relation between the average relative luminance Y_A and the illuminance L, the Y_A value of each sample image used for the CCMs calculation was calculated first. Then the illuminance is plotted with respect to Y_A in Fig. 4. A power function as in Eq. (9) was fitted to the plot in Fig. 4. The adoption of a power function is due to the fact that a digital image shall go through the gamma encoding, which is in a power-function form, before it can be correctly perceived by human eyes.

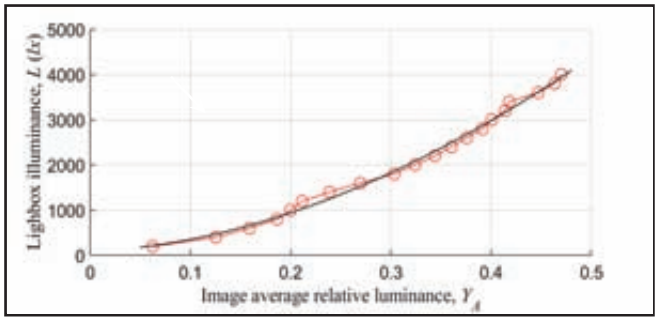

Figure 4. Variation of sample image relative luminance dependent on lightbox luminance

$$L = 7414 \cdot \left(Y_A\right)^{1.792} + 57.08 \tag{9}$$

Substituting Eq. (9) into Eq. (6), the relation between the CCMs and the average relative luminance of an image can be established.

D. Evaluation of Color Differences

The color accuracy of each color patch in the laparoscopic image can be evaluated by the CIE LAB color difference ΔE^*_{ab} [12]. The color difference ΔE^*_{ab} is given as follows.

$$\Delta E^*_{ab} = \sqrt{(\Delta L^*)^2 + (\Delta a^*)^2 + (\Delta b^*)^2} \tag{10}$$

Where the ΔL^*, Δa^* and Δb^* denote the errors between the detected colors and the reference colors in the CIE LAB color space. The conversion between the CIE LAB color space and the RGB color space was performed using the Imatest software.

III. Experiments and Discussions

A binocular high-definition (HD) laparoscope with a resolution of 1920 × 1080, as shown in Fig.1, was applied in the verification of the proposed method in this paper.

The results of the color correction on the images captured by the two laparoscopic cameras are very similar. Thus, in this paper, only the results from the left camera were analyzed and discussed. The sample images were captured at the illuminance levels as mentioned in Section II.B. The relation between the image average relative luminance value Y_A and the illuminance L is given in Section II.C.

The color correction validations were conducted on the laparoscopic images captured from i) the transmissive color target chart, ii) the X-Rite ColorChecker Classic Mini, and iii) the abdominal models, are reported in Section III.A, Section III.B, and Section III.C, respectively. Discussions about the experimental results are reported in Section III.D.

A. Color Correction on the Images Captured from the Transmissive Color Target

The illuminance of the lightbox was set at 400 lx, 800 lx, 1400 lx, 2600 lx, and 5000 lx, while the laparoscopic images were captured and subsequently corrected.

Figure 5 shows the comparison between the original laparoscopic images and its corrected ones. And Table I presents the results of the calculated illuminance from the image's average relative luminance, the color differences before and after correction.

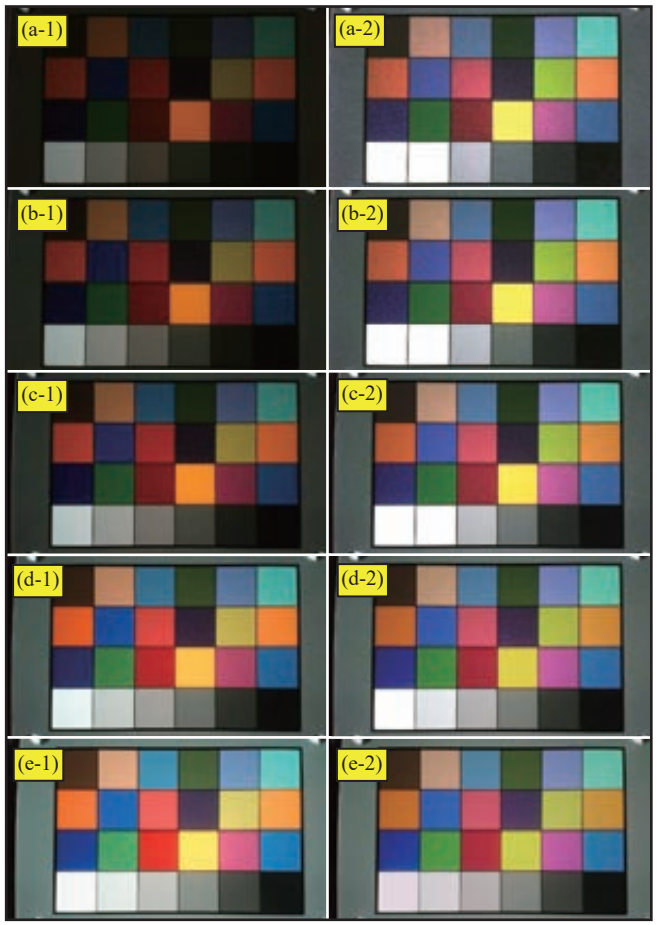

Figure 5. The laparoscopic images before (a-1)~(e-1) and after (a-2)~(e-2) color correction based on the proposed sample-based method. The images captured at illuminance levels of (a) 400 lx; (b) 800 lx; (c) 1400 lx; (d)2600 lx; and (e) 5000 lx

TABLE I. Calculated Relative Luminance And Color Difference Before And After Color Correction

Index	Actual L (Unit: lx)	Calculated L using the image luminance (Unit: lx)	Original ΔE^*_{ab}	Corrected ΔE^*_{ab}
(a)	400	473.6	47.1	16.4
(b)	800	844.4	36.9	14.8

(c)	1400	1257.7	29	13.9
(d)	2600	2677.0	16.1	10.4
(e)	5000	4063.2	14.8	9.7

As shown in Fig.5 and presented in Table I, the proposed sample-based color correction method is useful for reducing the color differences of the laparoscopic images captured from the transmissive color target chart. Although the original ΔE^*_{ab} of the images captured at low illuminance is substantially larger than that of the other images captured at higher illuminance, the color accuracy can be improved effectively. An improvement in terms of the color discrepancy of up to 65.18% was observed.

B. Color Correction on the Images Captured from the X-Rite Color- Checker Classic Mini

To further validate the method proposed in this paper, photos of an X-Rite ColorChecker Classic Mini color chart were captured and corrected, as shown in Fig.6. The color discrepancy of the images in Fig. 6(a-1) and Fig. 6(b-1) under office-environment lighting conditions before correction is 35.7 and 30.0, respectively. The average relative luminance of the images is 0.19 and 0.26, respectively, based on the luminance of the images' pixels. Then the illuminance of the images is estimated to be 839.2 lx and 1467.4 lx, using the curve fitting results in Eq. (9). Utilizing the CCMs under the corresponding illuminance, the color discrepancy was corrected to be 13.0 and 14.4, respectively. And the corrected images are shown in Fig. 6(a-2) and Fig. 6(b-2), respectively. The color discrepancy reduction is 63.6% and 52.0%.

Then, the utilized laparoscopic cameras were tilted to capture the images of the ColorChecker Classic Mini color chart in the tilted views to further validate the proposed sample-based approach, as in Fig.7. The original images are in Fig. 7(a-1) and Fig. 7(b-1) with the color discrepancy of 31.36 and 40.21, respectively. The corrected images in Fig. 7(a-2) and Fig. 7(b-2) have the color discrepancy reduced to 20.51 and 25.23, based on the entire images' luminance of 0.29 and 0.25. The Regions of Interest (ROIs) were extracted from Fig. 7(a-1) and Fig. 7(b-1) as in Fig. 7(a-3) and Fig. 7(b-3). And the images were cropped to show the corrected ROIs in Fig. 7(a-4) and Fig. 7(b-4). The color discrepancy was reduced to 13.59 and 13.99, based on the ROIs' luminance of 0.19 and 0.14. The results are also summarized in Table II.

Figure 6. Laparoscopic images of the X-Rite ColorChecker Classic Mini color chart (a-1)(b-1) before correction, and (a-2)(b-2) after correction

TABLE II. COLOR DIFFERENCES OF IMAGE CAPTURED WITH SLANTING DIRECTION

Image Stage	ΔE^*_{ab} in Fig.7(a)	ΔE^*_{ab} in Fig.7(b)
Original	31.36	40.21
Full frame luminance	0.29	0.25
Full frame correction	20.51	25.23
ROI luminance	0.19	0.14
ROI correction	13.59	13.99

Figure 7. Laparoscopic images of the X-Rite ColorChecker Classic Mini color chart in tilted views: (a-1)(b-1) the original images, (a-2)(b-2) the color-corrected ones based on the entire image's luminance; (a-3)(b-3) the ROI of the original images; (a-4)(b-4) the color-corrected ones of the cropped image based on the ROI's luminance.

From Table II, it is clear that the color discrepancy can be reduced by the proposed color correction approach. The outcomes were further improved by applying the proposed approach to the ROIs. Since this paper primarily investigates the color correction in low illumination scenarios, the use of the ROIs' luminance is clearly more effective in generating better color correction results.

C. Color Correction on the Images Captured from the Abdominal Models

The captured laparoscopic images of the abdominal models before and after color correction under different illumination conditions are shown in Fig.8. The image luminance of Fig. 8(a-1), Fig. 8(b-1), Fig. 8(c-1) and Fig. 8(d-1) is 0.06, 0.13, 0.14 and 0.11, respectively. The estimated illuminance is then 205.2 lx, 495.8 lx, 532.2 lx and 398.0 lx. Using the corresponding CCMs, the corrected images are shown in Fig. 8(a-2), Fig. 8(b-2), Fig. 8(c-2) and Fig. 8(d-2).

From the corrected images in Fig. 8, one can visually perceive the effectiveness of the proposed color correction approach. Particularly for the laparoscopic images captured under a dark surrounding, the color presentation and characteristics of the images are indeed improved.

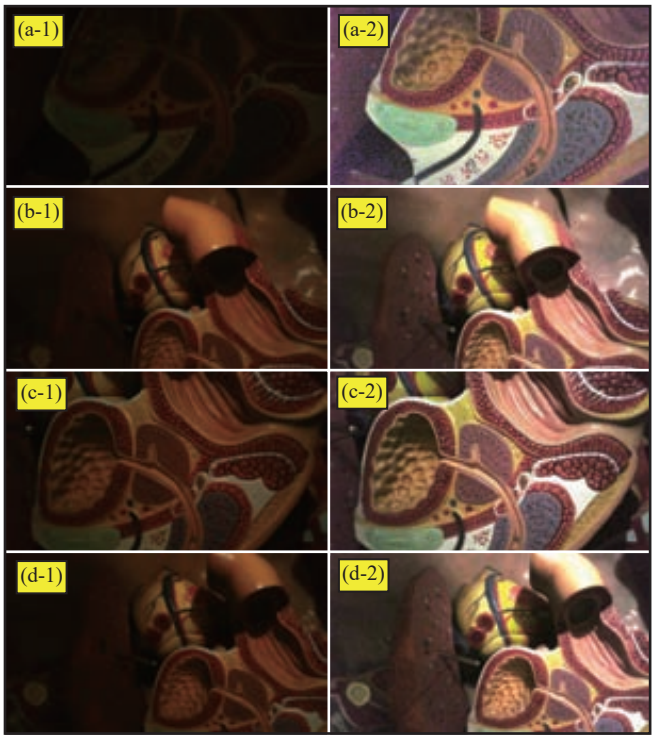

Figure 8. Laparoscopic images of the abdominal model: (a-1)~(d-1) before correction, and (a-2)~(d-2) after color correction.

D Discussions

The effectiveness of the proposed sample-based approach has been demonstrated by the conducted experimental investigations as presented in Sections III.A to III.C for the standard color charts and the abdominal models under various illuminance levels. In particular, for the images captured at low illuminance with possible loss of image details, the interpolated CCM can be used to effectively restore the color information and even other image features. For example, the image in Fig. 8(b-1) shows the model organs with an orange-like color. But color of the model organ is perceived red-like to human eyes under adequate illuminance. The corrected image in Fig. 8(b-2) was able to correct the presentation of the model organ color to a red-like appearance.

There are still some issues with the current results. Firstly, an overexposure may occur after the color correction, as shown in Fig. 8(b-2) and Fig. 8(d-2). Secondly, the image luminance outside the ROI (e.g, a dimmed background) will affect the entire image's luminance. The use of the image's overall luminance for color correction may be sub-optimal. These issues will be tackled in a future study.

On the other hand, the noise may seem to be increased after the color correction as in Fig. 8(a-2). However, this might be due to the fact that the noise in Fig. 8(a-1) may not be visible since the image is really dark. The proposed CCM is a linear color remapping method. It is not expected to change an image's noise level.

IV. Conclusion And Future Work

This paper presents a sample-based approach of the color correction for laparoscopic and endoscopic images. By correlating the average relative luminance of sample images and the sampled CCMs under different illuminance, an interpolated CCM is utilized for color correction for the laparoscopic image captured under various illumination conditions. Experimental verifications showed that the color discrepancy can be reduced up to 65.18% of the original color discrepancy before correction. The proposed approach is particularly useful for the laparoscopic images taken in low illumination scenarios. The outcome can be further improved if the proposed approach is applied on a focused ROI.

The proposed approach will be under further investigation for improvements primarily in the following two aspects. Firstly, overexposure should be taken into consideration for the color correction. The overexposure should be strictly limited if not totally avoided. Secondly, regionally smoothed CCM should be investigated for the color correction under non-uniform illumination. In this way, the ROI's color correction can be better performed using local, instead of overall, area luminance.

References

[1] R. H. Taylor, "A Perspective on Medical Robotics," *Proceedings of the IEEE,* Vol. 94, No.9, pp. 1652- 1664, 2006.

[2] J.-Y. Jang, "The Past, Present, and Future of Image-Enhanced Endoscopy," *Clinical Endoscopy,* Vol. 48, No.6, pp. 466-475, 2015.

[3] J. Penczek, P. A. Boynton, and J. D. Splett, "Color Error in the Digital Camera Image Capture Process," *Journal of Digital Imaging,* Vol. 27, No.2, pp. 182-191, 2014.

[4] F. Yaman, N. Bai, B. Zhu, T. Wang, and G. Li, "Long Distance Transmission in Few-Mode Fibers," *Optics Express,* Vol. 18, No.12, pp. 13250-13257, Jun 2010.

[5] R. M. Sousa, M. Wäny, P. Santos, and F. Morgado-Dias, "Automatic Illumination Control for An Endoscopy Sensor," *Microprocessors and Microsystems,* Vol. 72, No.2020, pp. 1-10, 2020.

[6] T. H. Khan, S. K. Mohammed, M. S. Imtiaz, and K. A. Wahid, "Color Reproduction and Processing Algorithm Based on Real-time Mapping for Endoscopic Images," *SpringerPlus,* Vol. 5, No.1, pp. 1-16, 2016.

[7] V. Cheung, S. Westland, D. Connah, and C. Ripamonti, "A Comparative Study of the Characterisation of Colour Cameras by Means of Neural Networks and Polynomial Transforms," *Coloration Technology,* Vol. 120, No.1, pp. 19-25, Jan 2004.

[8] G. Hong, M. R. Luo, and P. A. Rhodes, "A Study of Digital Camera Colorimetric Characterization Based on Polynomial Modeling," *Color Research & Application,* Vol. 26, No.1, pp. 76-84, 2001.

[9] G. D. Finlayson, M. Mackiewicz, and A. Hurlbert, "Color Correction Using Root-Polynomial Regression," *IEEE Transactions on Image Processing,* Vol. 24, No.5, pp. 1460-1470, 2015.

[10] W. Stephen, "Color Correction Matrix for Digital Still and Video Imaging Systems," National Telecommunications and Information Administration, Washington, DC TM-04-406, 2003.

[11] G. D. Finlayson, M. M. Darrodi, and M. Mackiewicz, "The Alternating Least Squares Technique for Nonuniform Intensity Color Correction," *Color Research & Application,* Vol. 40, No.3, pp. 232-242, 2015.

[12] J. Schanda, *Colorimetry: Understanding the CIE System*. Hoboken, New Jersey: John Wiley & Sons, Inc., 2007.

[13] J. Benesty, J. Chen, Y. Huang, and I. Cohen, "Pearson Correlation Coefficient," in *Noise Reduction in Speech Processing*, I. Cohen, Y. Huang, J. Chen, and J. Benesty, Eds. Berlin, Heidelberg: Springer, 2009, pp. 1-4

[14] R. Szeliski, *Computer Vision: Algorithms and Applications*. London: Springer-Verlag London Limited, 2011.